Electronic Supplementary Material (ESI) for Journal of Materials Chemistry B.
This journal is © The Royal Society of Chemistry 2019

Electronic Supplement Information

Reversible, switchable pH-driven quaternary ammonium pillar[5]arene nanogate for mesoporous silica nanoparticles

Evelyn C. S. Santos[a], Thiago C. dos Santos[a], Tamires S. Fernandes[a], Fernanda L. Jorge[c], Vanessa Nascimento[b], Vinícius G. C. Madriaga[a], Pâmella S. Cordeiro[b], Noemi R. Checca[d], Nathalia Meireles Da Costa[c], Luís Felipe R. Pinto[c], and Célia M. Ronconi*[a]

[a]*Departamento de Química Inorgânica and* [b]*Departamento de Química Orgânica, Universidade Federal Fluminense (UFF), Niterói, RJ, Brazil*

[c]*Molecular Carcinogenesis Program, Instituto Nacional de Câncer (INCA), Rio de Janeiro, RJ, Brazil*

[d]*Centro Brasileiro de Pesquisas Físicas (CBPF), Rio de Janeiro-RJ, Brazil.*

*E-mail: cmronconi@id.uff.br

Table of contents

Scheme S1. Synthetic rote employed to obtain water-soluble P[5]A……..... S5

Figure S1. ^{1}H NMR spectra of: (a) compound **2** ($CDCl_3$, RT, 500 MHz) and (b) P[5]A (D_2O, RT, 500 MHz).....…….. S6

Figure S2. ^{13}C NMR spectrum of the P[5]A (D_2O, RT, 75 MHz)……. S7

Figure S3. FTIR spectra of the MCM-41-COOH and its precursors……... S7

Figure S4. Raman spectra of MCM-41-COOH and MCM-41-CN…….. S8

Figure S5. N_2 Adsorption and desorption isotherms of MCM-41, MCM-41-COOH, MCM-41-COO-DOX-P[5]A, MCM-41-DOX-P[5]A, MCM-41-P[5]A and MCM-41-COO-P[5]A measured at 77 K. Adsorption = closed cycle, desorption = open cycle……..……..... S8

Figure S6. BJH pore size distributions of MCM-41, MCM-41-COOH, MCM-41-COO-DOX-P[5]A, MCM-41-DOX-P[5]A, MCM-41-P[5]A and MCM-41-COO-P[5]A obtained from adsorption branch…….. S9

Table S1. Textural properties of the DOX-unloaded and DOX-loaded materials……... S9

Figure S7. PXRD patterns of MCM-41 and MCM-41-COOH…….. S10

Figure S8. (a) Scanning electron microscopy (SEM), (b) particle size distribution (PSD) and (c, d) transmission electron microscopy (TEM) of MCM-41….....……. S10

Figure S9. TEM images of MCM-41-COOH obtained at different scale of size…… S11

Figure S10. Dynamic light scattering distribution (DLS) of (a) MCM-41 and (b) MCM-41-COOH.....……..... S11

Figure S11. ζ-potential curves as a function of pH (2-11) for MCM-41 and MCM-41-COOH in PBS buffer at RT……..…….. S12

Figure S12. Acid-base titration curves of the MCM-41 and MCM-41-COOH……. S12

Figure S13. Gran plots for (a) MCM-41 and (b) MCM-41-COOH.[1,2] The curves were obtained by plotting the Gran function (V_{NaOH} x 10^{-pH}), *i.e.*, the product of NaOH volume added and the antilog of the pH as a function of NaOH volume used in the titration (Fig. S9). The intersections of the red lines in the V_{NaOH}-axis (when y = 0) provide the equivalence volumes of the base necessary to completely react with all acid sites. These volumes were used to calculate the concentrations of acid sites in MCM-41 and MCM-41-COOH. The protonation constants (pK_a) for both materials were obtained from the slope of the red line…… S13

Table S2. Protonation constant (pK_a) and concentration of the acid sites in the MCM-41 and

MCM-41-COOH determined by Gran Method…….. S13

Figure S14. FTIR spectra of the MCM-41-P[5]A, MCM-41-COO-P[5]A, P[5]A and MCM-41-COOH.....……..... S14

Figure S15. Optimized structure of P[5]A. The structure was optimized using the Chem3D module available in Chem3DUltra…..... S14

Figure S16. (a) Absorption spectra of DOX at different concentrations in PBS solution (pH = 7.4) obtained at RT and (b) the standard curve of DOX obtained from the absorption spectra using the absorption maximum at λ = 483 nm. This standard curve was used to estimate the amount of doxorubicin loaded and released from the nanocarriers……... S15

Figure S17. The UV-Vis spectra of DOX released in PBS solution over time, at 37 ^{o}C for MCM-41-DOX-P[5]A at (a) pH = 2.0, (c) pH = 5.5 and (e) pH = 7.4; and for MCM-41-COO-DOX-P[5]A at (b) pH = 2.0, (d) pH = 5.5, (f) pH = 7.4..... S16

Figure S18. The UV-Vis spectra of DOX released for MCM-41-COO-DOX-P[5]A after consecutive additions of acid and base to a suspension of the nanocarrier in PBS at 37 °C at (a) pH = 5.5, (b) pH = 2.0..... S17

Figure S19. The UV-Vis spectra of DOX released for MCM-41-COO-DOX-P[5]A over time after addition of (a) 1.2 mmol L^{-1} Zn^{2+}, (b) 50 mmol L^{-1} Zn^{2+} (c) 19 mmol L^{-1} $citrate^{3-}$ in PBS solution at 37 °C..... S18

Figure S20. MTT viability assay of MCF-7 cells treated with DOX-unloaded MCM-41-COO-P[5]A for 24 and 48 h using the concentrations of 0.5, 1.0, 2.5 and 5.0 μg mL^{-1} of the nanocarrier..... S19

Figures, Schemes and Tables

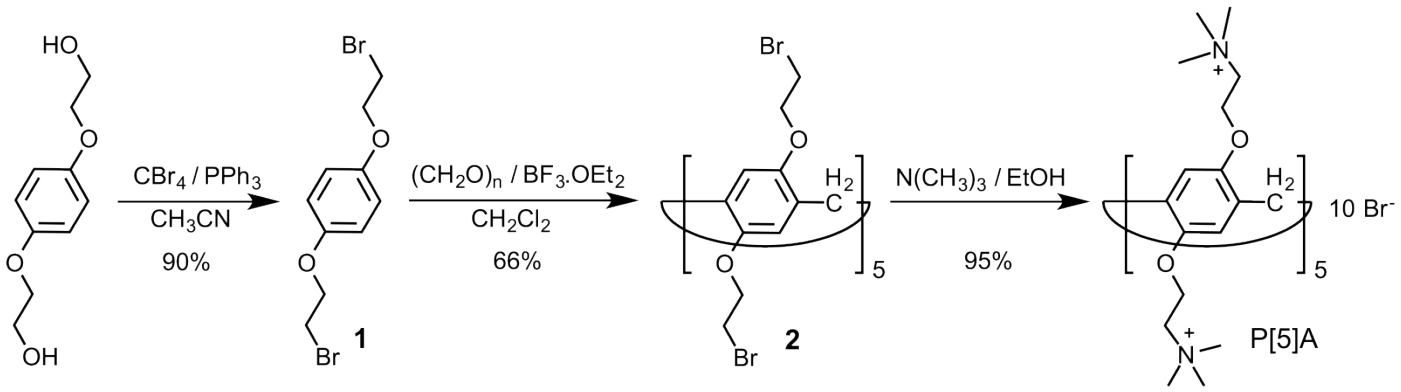

Scheme S1. Synthetic rote employed to obtain water-soluble P[5]A.

(a)

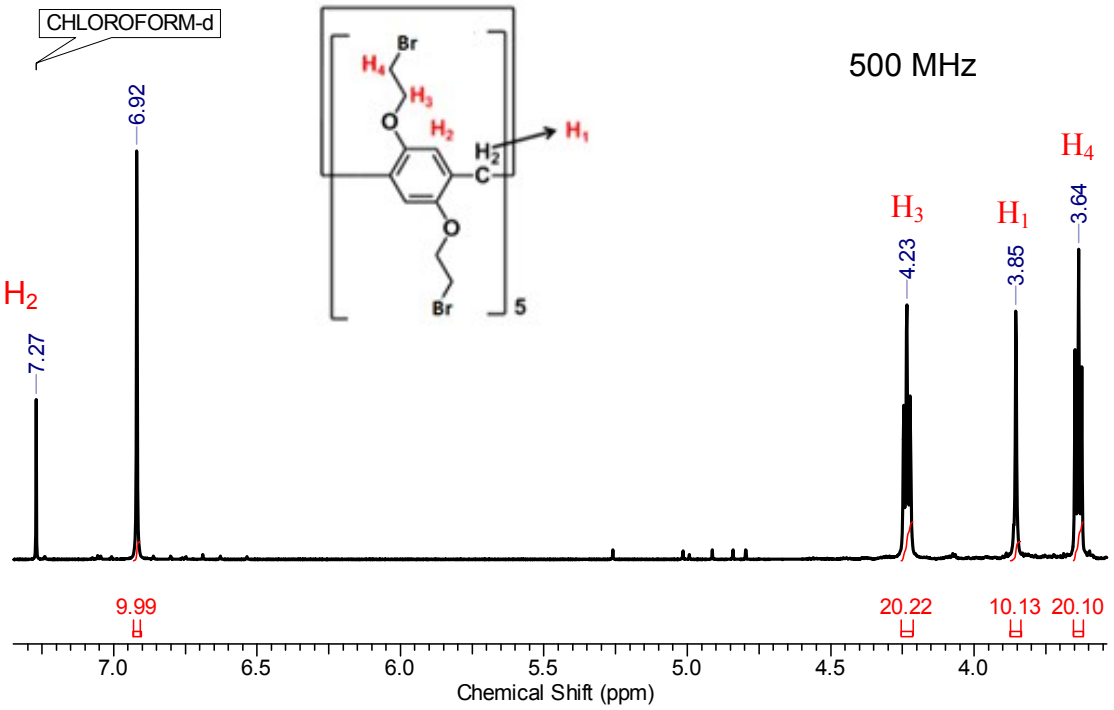

(b)

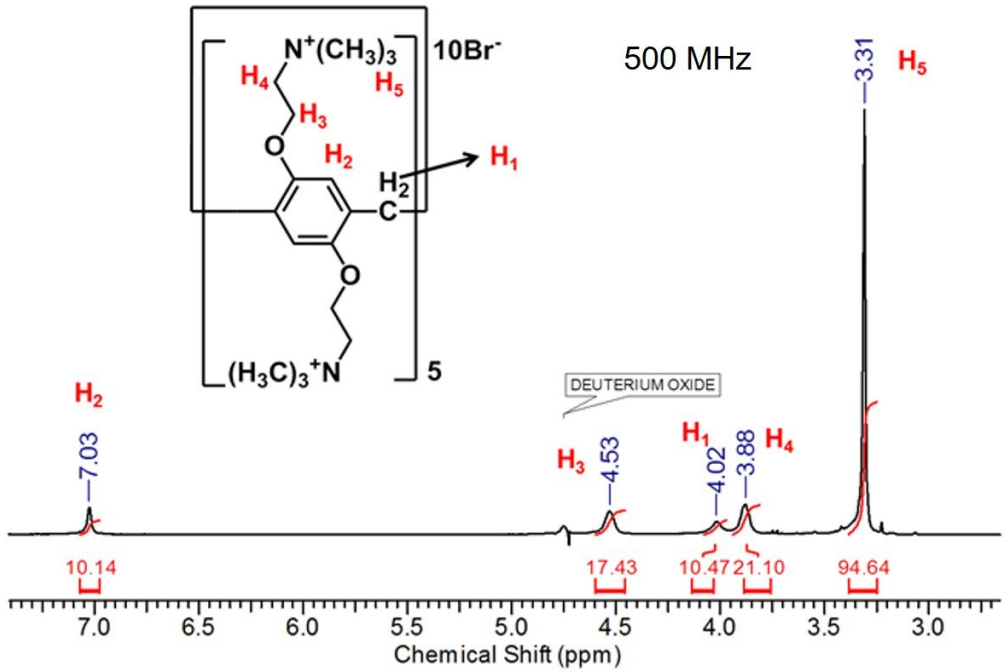

Figure S1. ^{1}H NMR spectra of: (a) compound **2** ($CDCl_3$, RT, 500 MHz) and (b) P[5]A (D_2O, RT, 500 MHz).

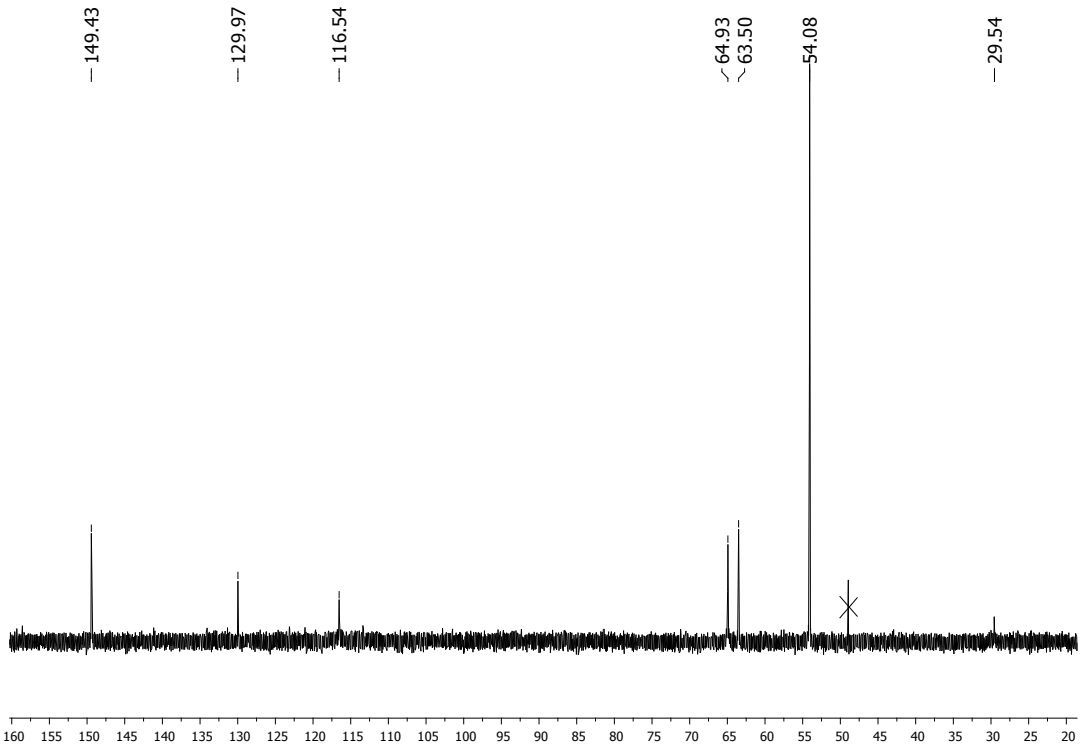

Figure S2. ^{13}C NMR spectrum of the P[5]A (D_2O, RT, 75 MHz).

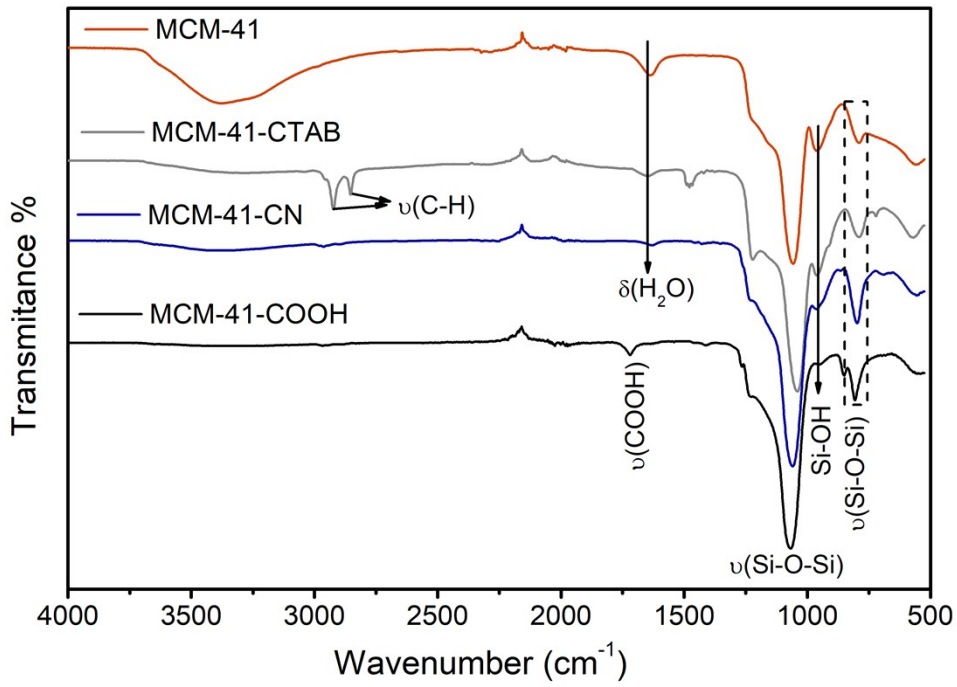

Figure S3. FTIR spectra of the MCM-41-COOH and its precursors.

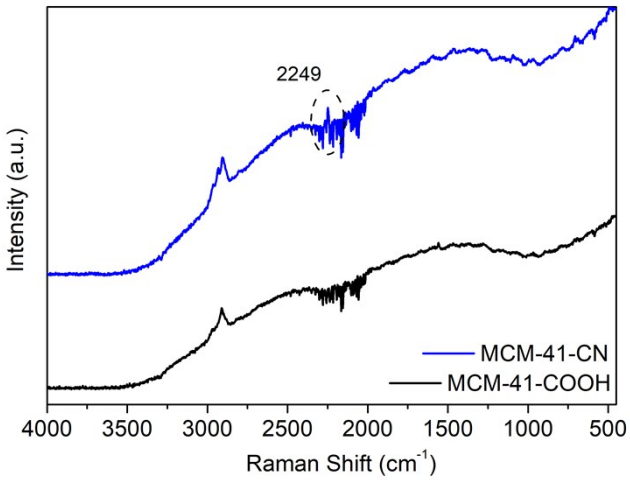

Figure S4. Raman spectra of MCM-41-COOH and MCM-41-CN.

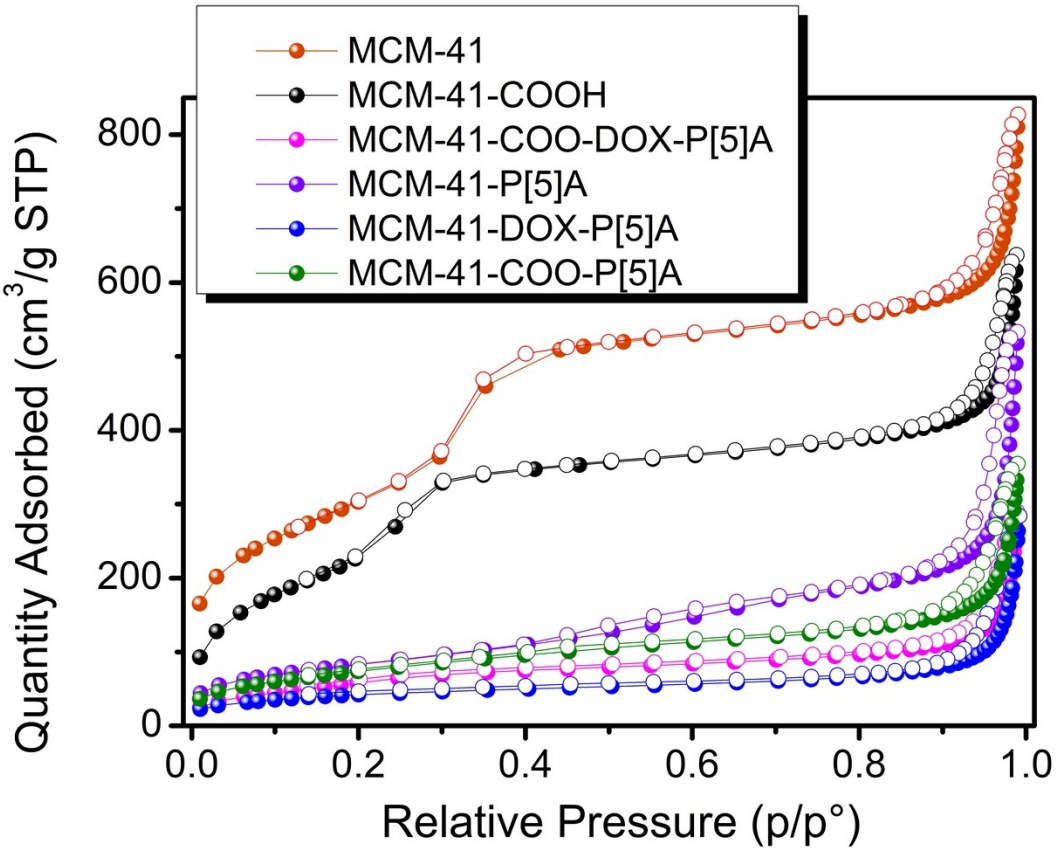

Figure S5. N_2 Adsorption and desorption isotherms of MCM-41, MCM-41-COOH, MCM-41-COO-DOX-P[5]A, MCM-41-DOX-P[5]A, MCM-41-P[5]A and MCM-41-COO-P[5]A measured at 77 K. Adsorption = closed cycle, desorption = open cycle.

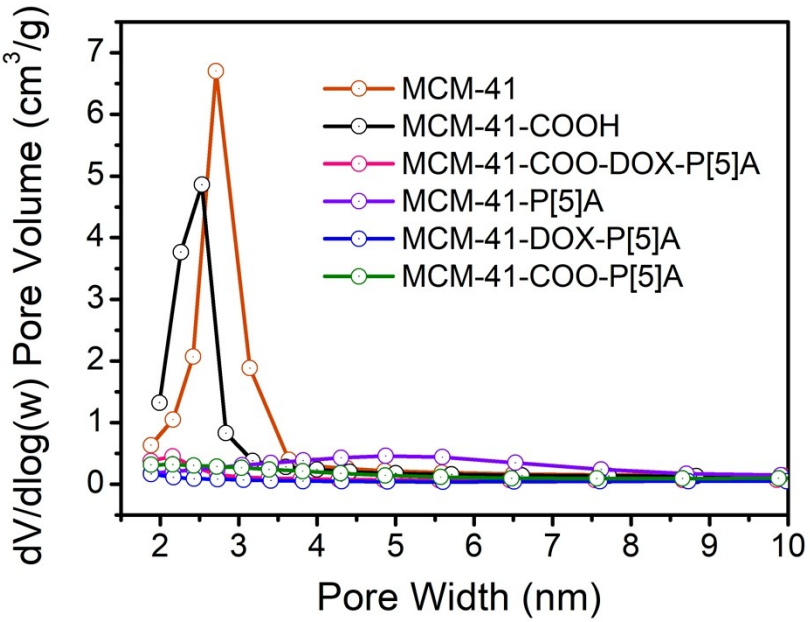

Figure S6. BJH pore size distributions of MCM-41, MCM-41-COOH, MCM-41-COO-DOX-P[5]A, MCM-41-DOX-P[5]A, MCM-41-P[5]A and MCM-41-COO-P[5]A obtained from adsorption branch.

Table S1. Textural properties of the DOX-unloaded and DOX-loaded materials.

Materials	BET surface area (m^2 g^{-1})	BJH adsorption cumulative volume of pores V_p (cm^3 g^{-1})	BJH adsorption pore diameter (nm)
MCM-41	1034	1.14	2.72
MCM-41-COOH	755	0.97	2.54
MCM-41-COO-P[5]A	234	-	-
MCM-41-COO-DOX-P[5]A	188	-	-
MCM-41-P[5]A	284	-	-
MCM-41-DOX-P[5]A	144	-	-

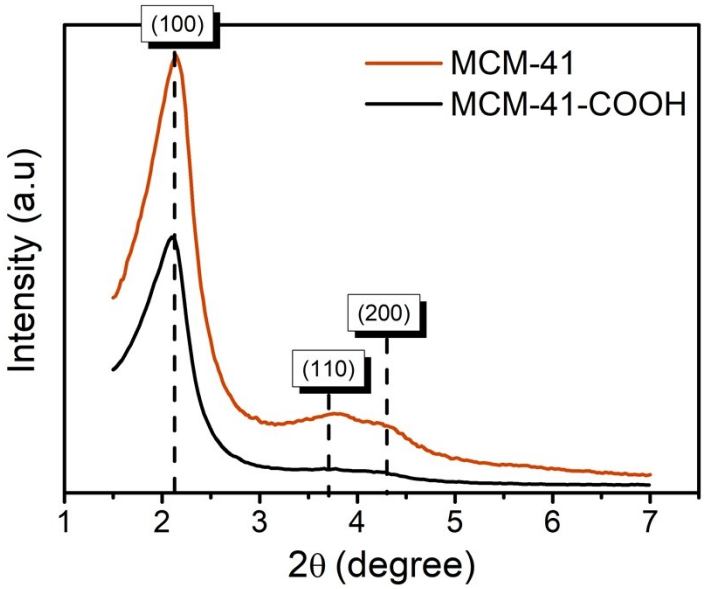

Figure S7. PXRD patterns of MCM-41 and MCM-41-COOH.

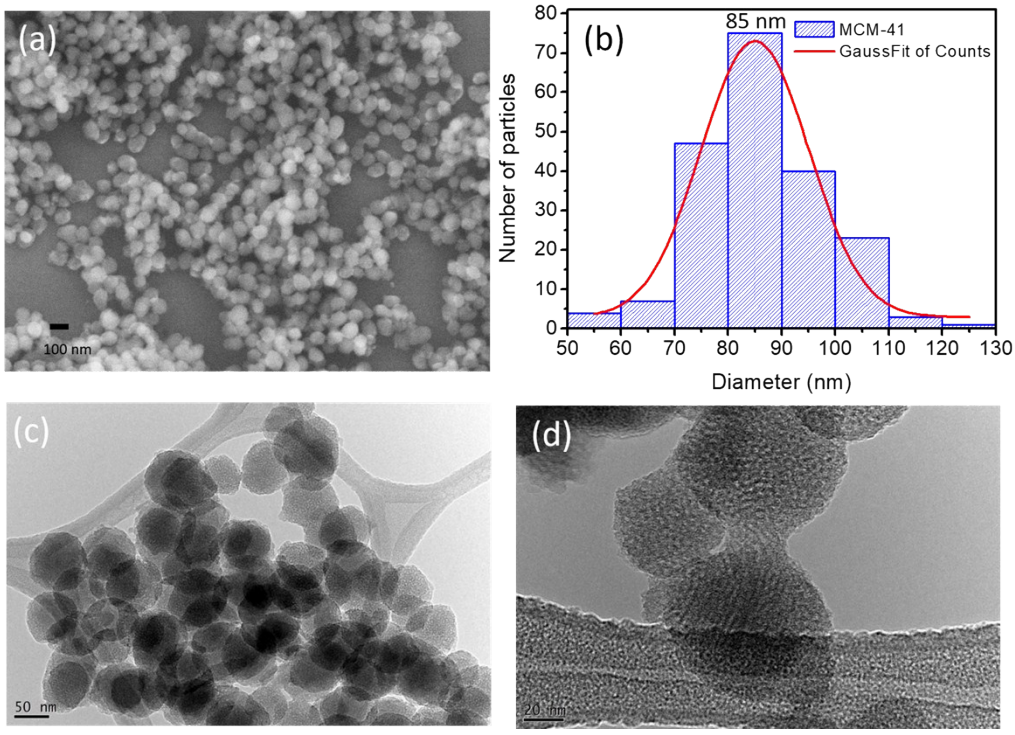

Figure S8. (a) Scanning electron microscopy (SEM), (b) particle size distribution (PSD) and (c, d) transmission electron microscopy (TEM) of MCM-41.

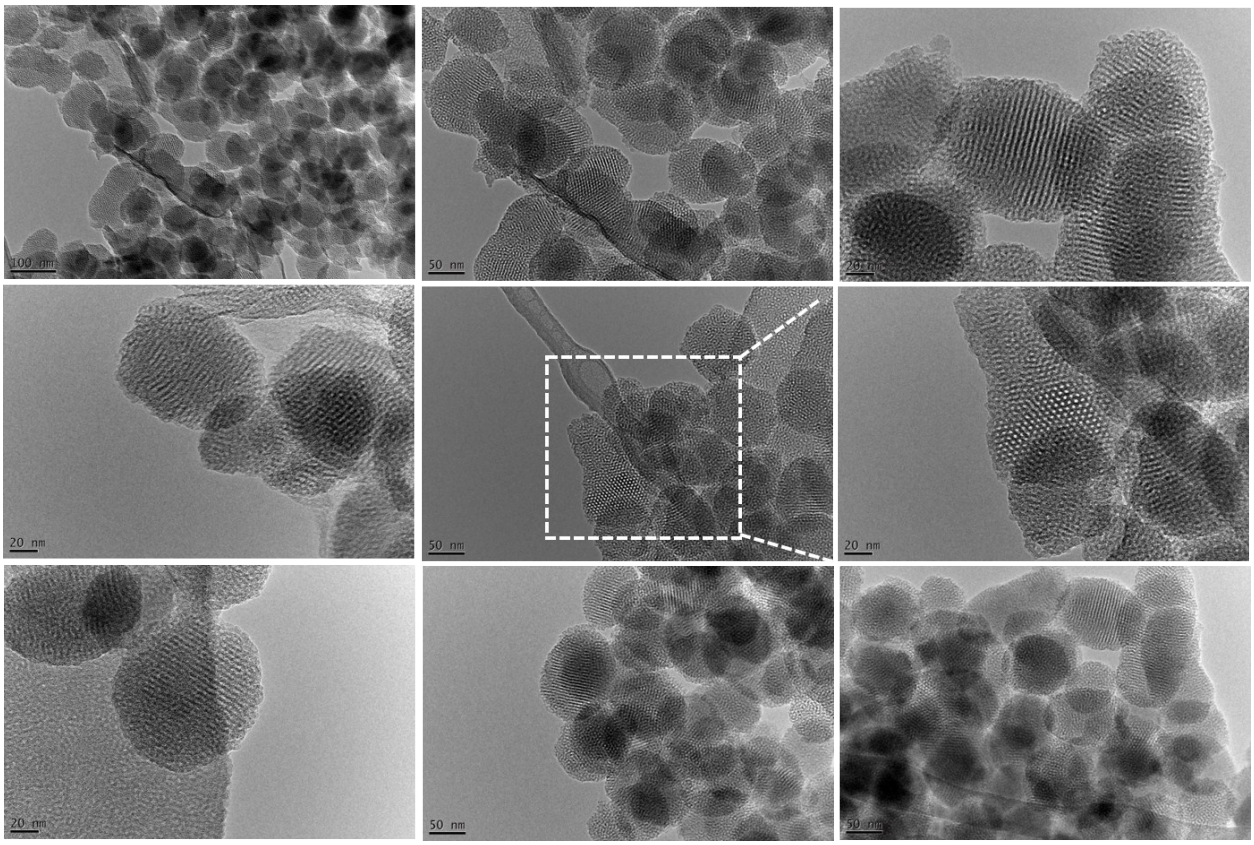

Figure S9. TEM images of MCM-41-COOH obtained at different scale of size.

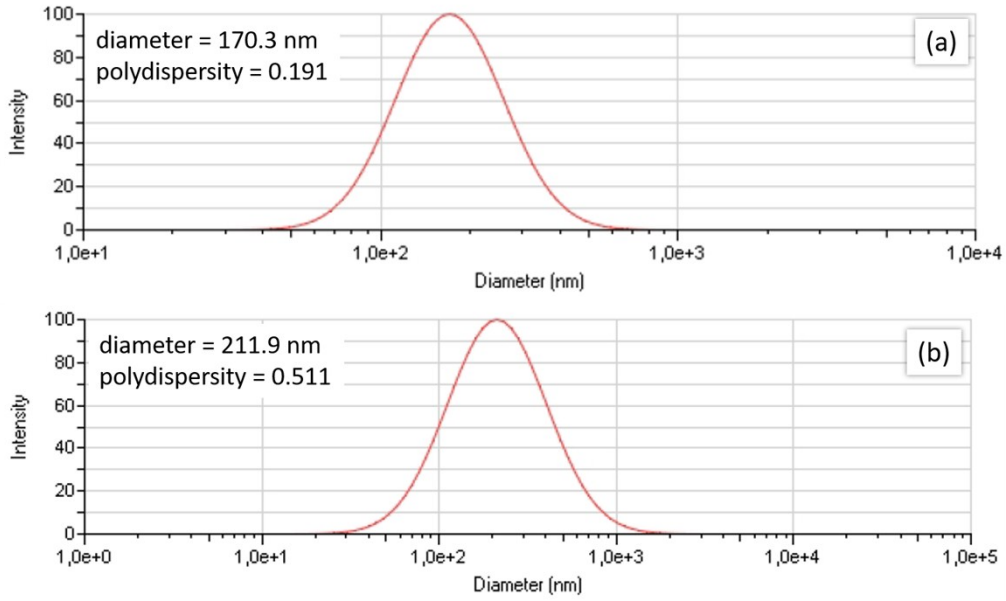

Figure S10. Dynamic light scattering distribution (DLS) of (a) MCM-41 and (b) MCM-41-COOH in deionized water.

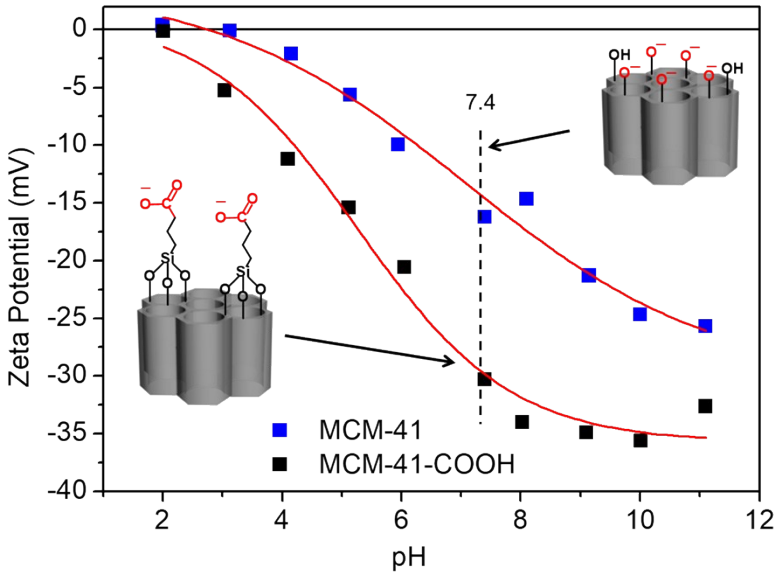

Figure S11. ζ-potential curves as a function of pH (2-11) for MCM-41 and MCM-41-COOH in PBS buffer at RT.

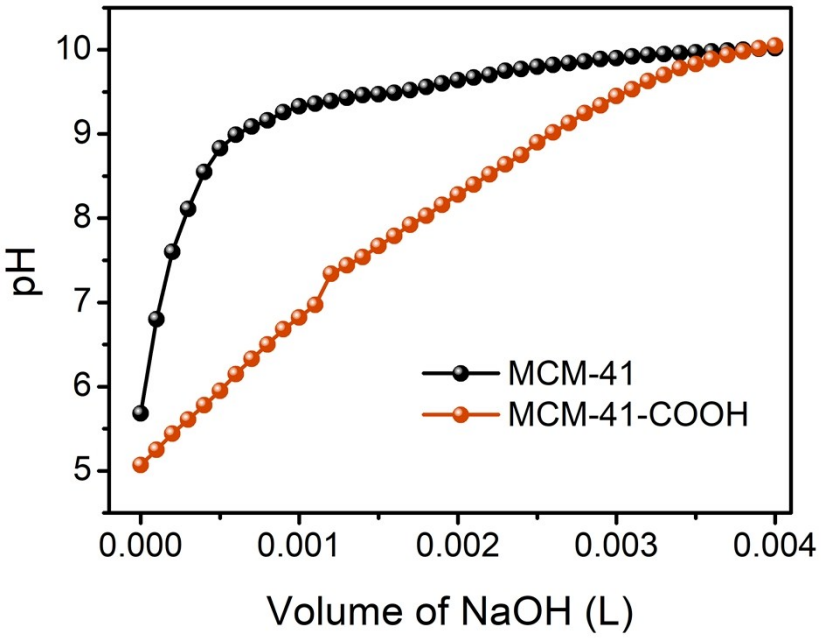

Figure S12. Acid-base titration curves of the MCM-41 and MCM-41-COOH.

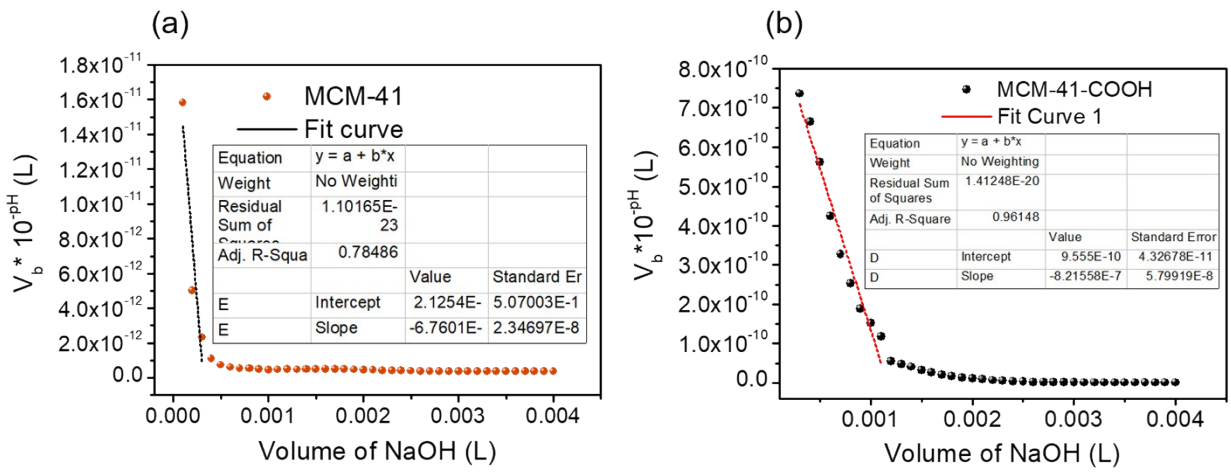

Figure S13. Gran plots for (a) MCM-41 and (b) MCM-41-COOH.[1,2] The curves were obtained by plotting the Gran function (V_{NaOH} x 10^{-pH}), *i.e.*, the product of NaOH volume added and the antilog of the pH as a function of NaOH volume used in the titration (Fig. S12). The intersections of the red lines in the V_{NaOH}-axis (when y = 0) provide the equivalence volumes of the base necessary to completely react with all acid sites. These volumes were used to calculate the concentrations of acid sites in MCM-41 and MCM-41-COOH. The protonation constants (pK_a) for both materials were obtained from the slope of the red line.

Table S2. Protonation constant (pK_a) and concentration of the acid sites in the MCM-41 and MCM-41-COOH determined by Gran Method.

Materials	pKa	Concentration of the acid sites (μmol g^{-1})
MCM-41	7.2	154
MCM-41-COOH	6.1	582

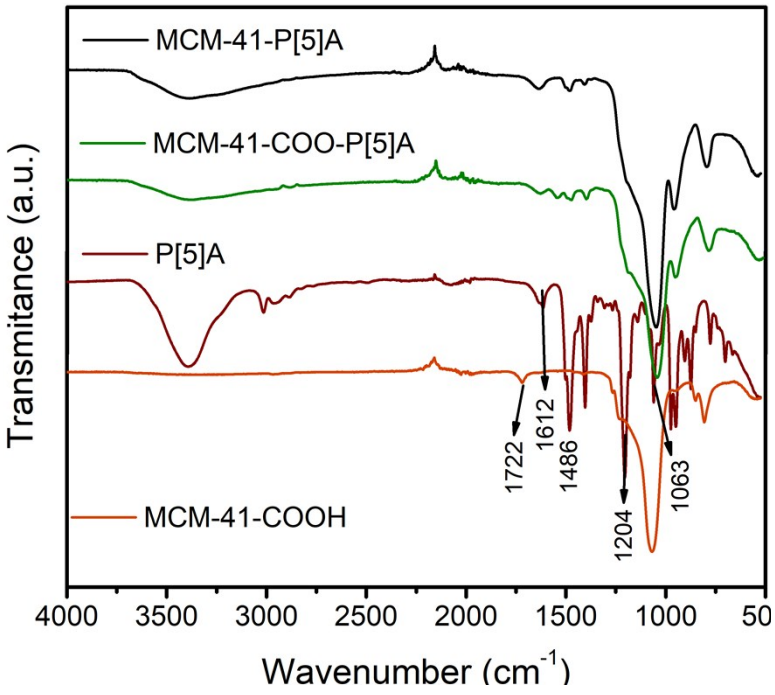

Figure S14. FTIR spectra of the MCM-41-P[5]A, MCM-41-COO-P[5]A, P[5]A and MCM-41-COOH.

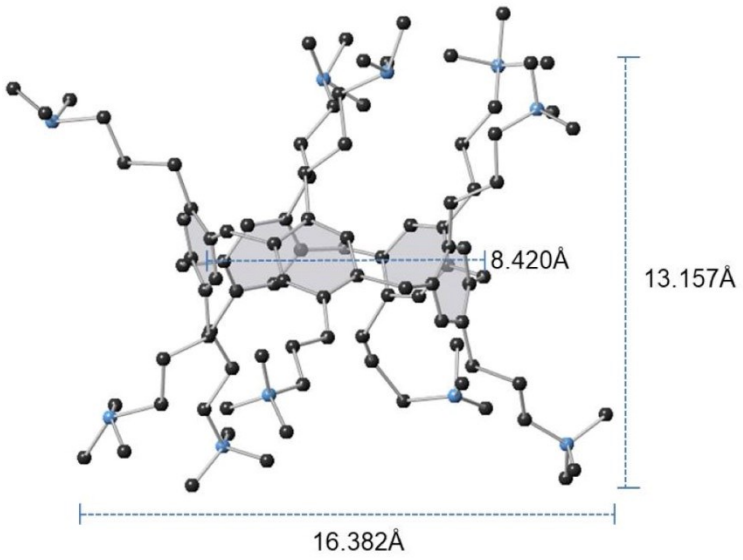

Figure S15. Optimized structure of P[5]A. The structure was optimized using the Chem3D module available in Chem3DUltra.

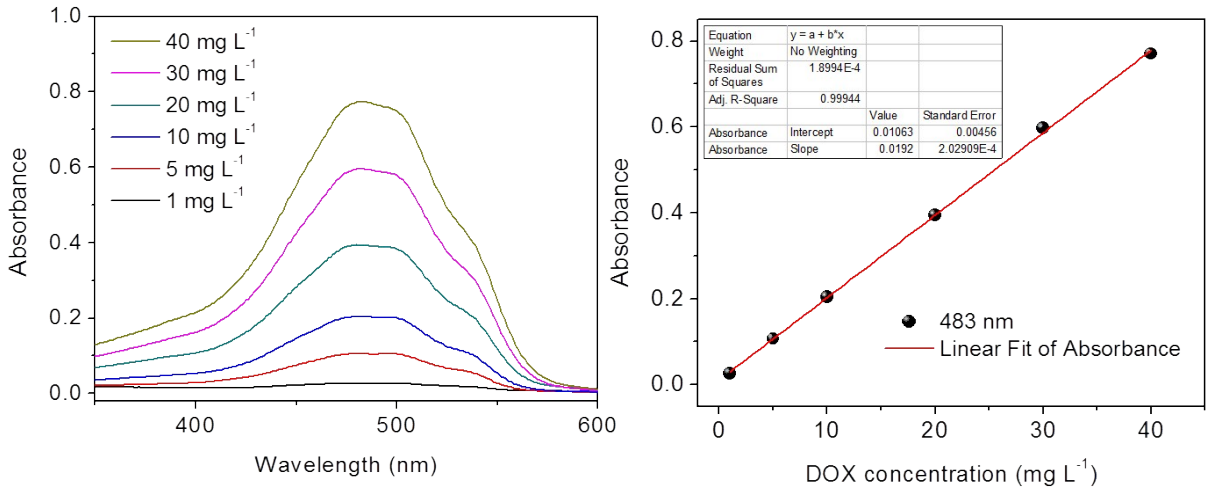

Figure S16. (a) Absorption spectra of DOX at different concentrations in PBS solution (pH = 7.4) obtained at RT and (b) the standard curve of DOX obtained from the absorption spectra using the absorption maximum at λ = 483 nm. This standard curve was used to estimate the amount of DOX loaded and released from the nanocarriers.

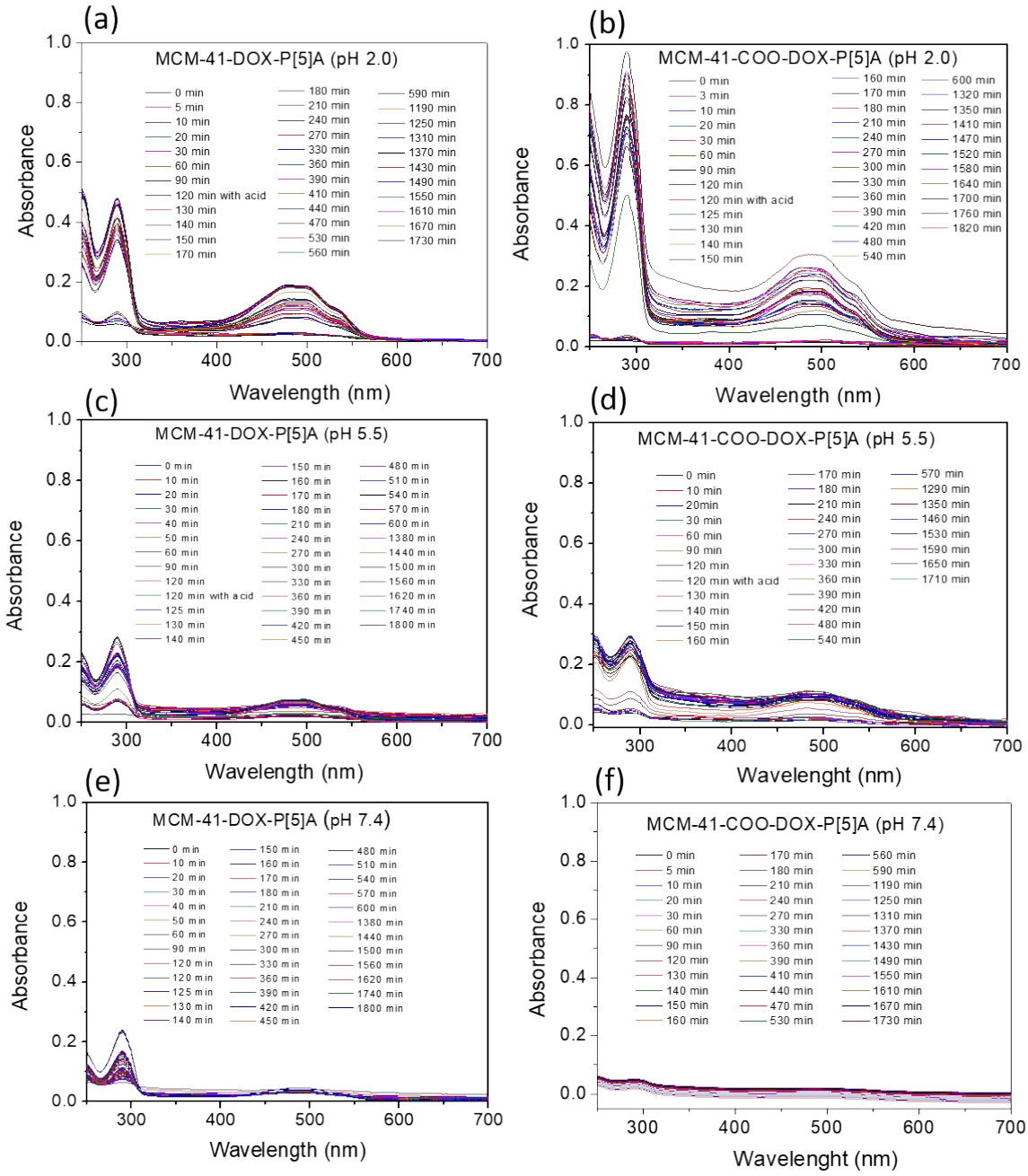

Figure S17. The UV-Vis spectra of DOX released in PBS solution over time, at 37 ^{o}C for MCM-41-DOX-P[5]A at (a) pH = 2.0, (c) pH = 5.5 and (e) pH = 7.4; and for MCM-41-COO-DOX-P[5]A at (b) pH = 2.0, (d) pH = 5.5, (f) pH = 7.4.

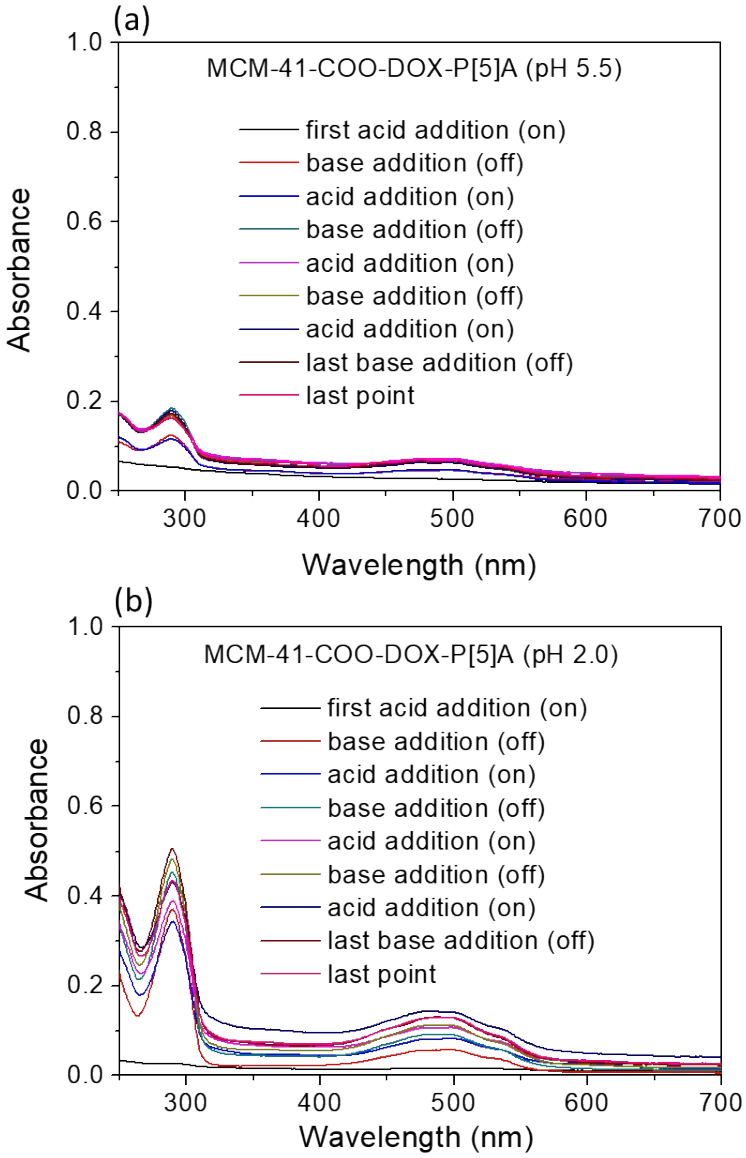

Figure S18. The UV-Vis spectra of DOX released for MCM-41-COO-DOX-P[5]A after consecutive additions of acid and base to a suspension of the nanocarrier in PBS at 37 °C at (a) pH = 5.5, (b) pH = 2.0.

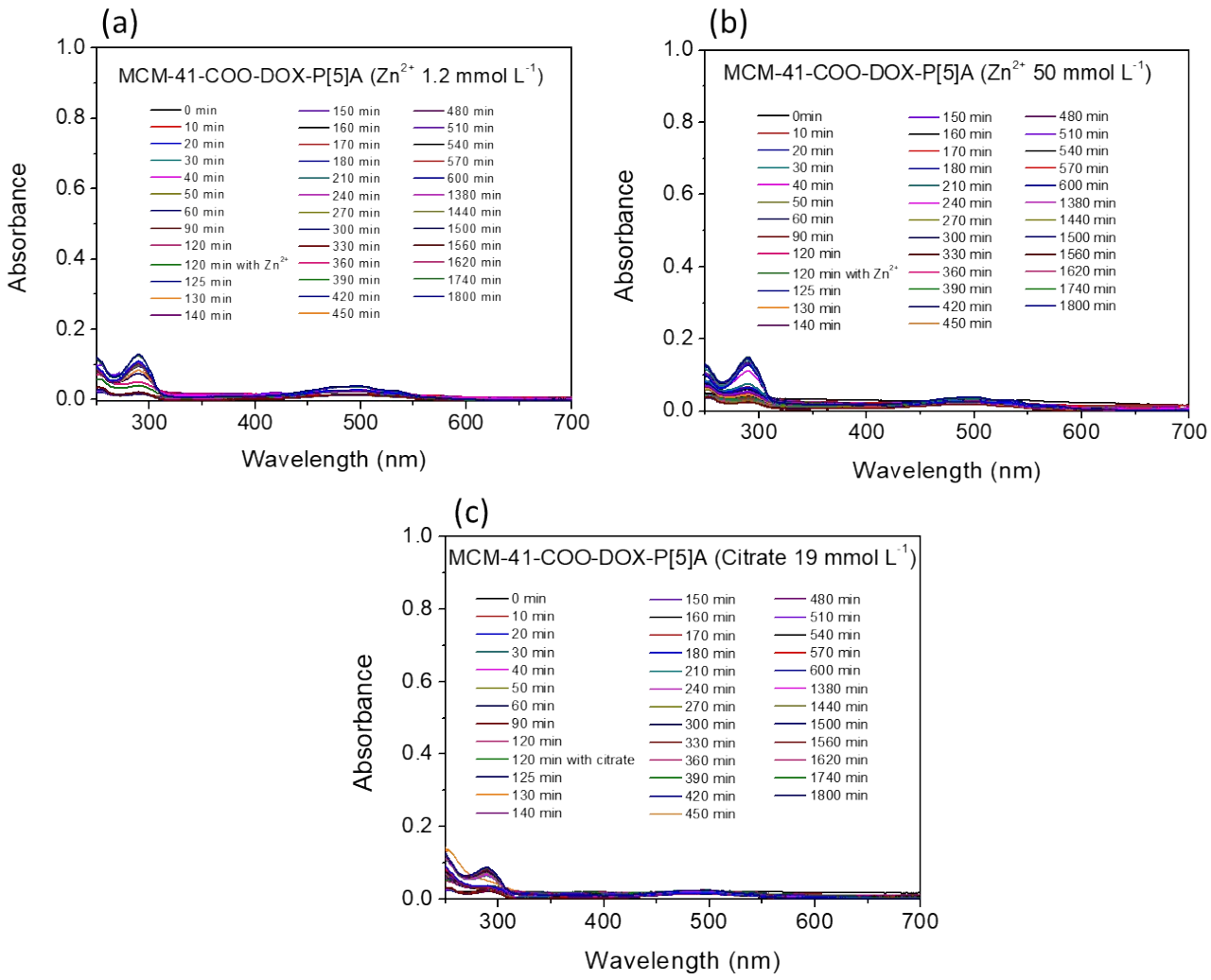

Figure S19. The UV-Vis spectra of DOX released for MCM-41-COO-DOX-P[5]A over time after addition of (a) 1.2 mmol L^{-1} Zn^{2+}, (b) 50 mmol L^{-1} Zn^{2+} (c) 19 mmol L^{-1} $citrate^{3-}$ in PBS solution at 37 °C.

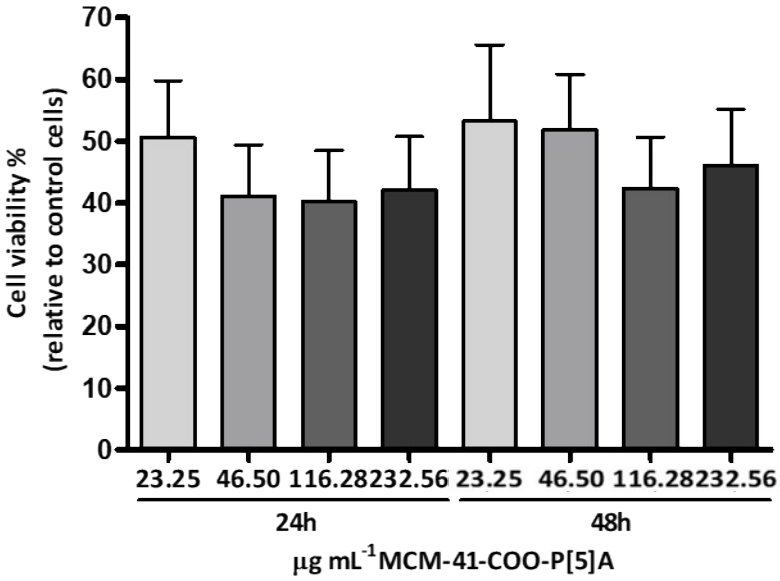

Figure S20. MTT viability assay of MCF-7 cells treated with DOX-unloaded MCM-41-COO-P[5]A for 24 and 48 h using the concentrations of 23.25, 46.50, 116.28 or 232.56 µg mL^{-1} of the nanocarrier.

References

(1) Yu, K.; Kumar, N.; Aho, A.; Roine, J.; Heinmaa, I.; Murzin, D. Y.; Ivaska, A. Determination of Acid Sites in Porous Aluminosilicate Solid Catalysts for Aqueous Phase Reactions Using Potentiometric Titration Method. *J. Catal.* **2016**, *335*, 117–124.

(2) Shcherban, N. D.; Filonenko, S. M.; Barakov, R. Y.; Sergiienko, S. A.; Yu, K.; Heinmaa, I.; Ivaska, A.; Murzin, D. Y. New Insights in Evaluation of Acid Sites in Micro-Mesoporous Zeolite-like Materials Using Potentiometric Titration Method. *Appl. Catal. A, Gen.* **2017**, *543*, 34–42.